NASA Technical Memorandum 88327

Influence of Dynamic Inflow on the Helicopter Vertical Response

Robert T.N. Chen and William S. Hindson

June 1986

National Aeronautics and
Space Administration

NASA Technical Memorandum 88327

Influence of Dynamic Inflow on the Helicopter Vertical Response

Robert T. N. Chen, Ames Research Center, Moffett Field, CA
William S. Hindson, Stanford University, Stanford, CA

June 1986

National Aeronautics and
Space Administration

Ames Research Center
Moffett Field, California 94035

INFLUENCE OF DYNAMIC INFLOW ON THE HELICOPTER VERTICAL RESPONSE

Robert T. N. Chen

NASA Ames Research Center, Moffett Field, CA 94035, USA

and

William S. Hindson

Stanford University, Stanford, CA 94305, USA

April 1986

Abstract--A study has been conducted to investigate the effects of dynamic inflow on rotor-blade flapping and vertical motion of the helicopter in hover. Linearized versions of two dynamic inflow models, one developed by Carpenter and Fridovich and the other by Pitt and Peters, were incorporated in simplified rotor-body models and were compared for variations in thrust coefficient and the blade Lock number. In addition, a comparison was made between the results of the linear analysis, and the transient and frequency responses measured in flight on the CH-47B variable-stability helicopter. Results indicate that the correlations are good, considering the simplified model used. The linear analysis also shows that dynamic inflow plays a key role in destabilizing the flapping mode. The destabilized flapping mode, along with the inflow mode that the dynamic inflow introduces, results in a large initial overshoot in the vertical acceleration response to an abrupt input in the collective pitch. This overshoot becomes more pronounced as either the thrust coefficient or the blade Lock number is reduced. Compared with Carpenter's inflow model, Pitt's model tends to produce more oscillatory responses because of the less stable flapping mode predicted by it.

NOMENCLATURE

a	slope of the lift curve (rad^{-1})
a_z	vertical acceleration of the aircraft (ft/s^2)
C_o	factor to account for dynamic inflow models used ($C_o = 1$ for Pitt model, $C_o = 0.639$ for Carpenter model)
C_T	thrust coefficient ($C_T = T/\rho\pi R^2(\Omega R)^2$)
c	blade chord (ft)
I_β	blade moment of inertia about flapping hinge ($slug\text{-}ft^2$)
M_β	blade mass-moment about the flapping hinge (slug-ft)

m mass of the total aircraft (slug)

m_a apparent additional air mass, $m_a = 0.637\rho(4/3)\pi R^3$ (slug)

N number of blades

R rotor radius (ft)

s Laplace transform variable

T thrust (lb)

v inflow perturbation (ft/s, positive downward)

w perturbation in aircraft vertical velocity (ft/s, positive downward)

w_o initial steady vertical velocity of the aircraft (ft/s)

Δ $1 - NM_\beta^2/mI_\beta$

γ blade Lock number ($\gamma = \rho acR^4/I_\beta$)

$\bar{v}_o$ inflow ratio ($\bar{v}_o = + (C_{T_o}/2)^{1/2}$)

Ω rotor angular velocity (rad/s)

σ rotor solidity ratio

β blade flapping angle (rad, positive upward)

ρ air density (slug/ft^3)

$\bar{v}$ $v/\Omega R$

$(\dot{x})$ time rate of change of x

$(\tilde{x})$ perturbation of x

θ_o collective pitch (rad)

δ_c collective stick displacement (in.)

1. INTRODUCTION

There is a trend toward using superaugmented, high-gain flight control systems [1,2] for the military rotorcraft in order to meet the requirements for demanding mission tasks such as nap-of-the-Earth (NOE) flight or aerial combat. In the design analysis of such high-gain control systems, it is now

essential that high-order dynamics of the system components be adequately modeled, in contrast to past practice when only the lower frequency, quasi-static, rigid body flight dynamics were used in the design of low-gain flight control systems. The requirement for adequate modeling of the high-order dynamics for high-gain flight control systems used in rotorcraft was found, for example, in recent flight investigations using a variable-stability research helicopter [3,4]. These investigations showed that, not only high-order elements such as rotor dynamics are required (Miller [5], Ellis [6], and Hall and Bryson [7]), but other high-order effects such as dynamics of sensor filters, servo actuators, and data processing delays of the airborne computer must also be adequately modeled.

Inclusion of air-mass dynamics associated with a lifting rotor may also prove to be important in the design of a high-gain flight control system for rotorcraft. Recent research [8-12] in dynamic inflow has shown that the frequencies of the inflow dynamic modes are the same order of magnitude as those of the rotor blade flapping and lead-lag modes, and as such, the dynamic inflow has a significant influence on the aeromechanic stability of the rotor system. These research efforts have focused mainly on the ground- and air-resonance problems, and have been concerned with the inflow dynamics associated with the pitch and roll motions of the rotor hub. Little has been done, however, since the original work of Carpenter and Fridovich [13] that has considered the interaction of dynamic inflow, rotor-blade flapping, and the vertical motion of the helicopter. These items are of particular interest in flight dynamics and control associated with such high bandwidth NOE tasks as rapid masking and unmasking vertical maneuvers.

In 1953, Carpenter and Fridovich [13] proposed a nonlinear dynamic inflow model to investigate the transient rotor thrust and the inflow buildup during

a jump take-off maneuver. The model permitted calculations of the responses of inflow, flapping, and thrust to large inputs in collective pitch. The results of calculations were in good agreement with the experimental test data obtained from a helicopter test stand with no aircraft motions. The inflow transient was found to exist for less than 1 sec after the blade pitch reaches its final value; the thrust overshoot was calculated to be about 100% (some 10% greater than measured) following a very rapid pitch increase. The nonlinear dynamic model that they proposed, while convenient for nonlinear simulation, provides little insight into the influence of the operational conditions (such as thrust coefficient), and the mass and inertia properties of the rotor blade on the thrust response and helicopter vertical motion.

This paper discusses the results of linear analyses conducted to gain better insight into these parametric effects. The use of linear analysis also expedites the development of a simplified mathematical model for use in the design analysis of high-bandwidth control systems for rotorcraft. One such linear analysis was conducted based on the nonlinear dynamic inflow model of Carpenter and Fridovich [13]. A nonlinear version of the Pitt-Peters dynamic inflow model [11,12] which was developed recently based on unsteady actuator-disc theory, was also linearized and incorporated into a simple rotor model [14,15] for a comparative investigation which included variations in thrust coefficient and the rotor-blade Lock number to assess the effect of dynamic inflow on the thrust response and helicopter vertical motion.

The remainder of this paper is organized as follows. First, the development of the linear equations of motion for the dynamic inflow, flapping, and vertical response characteristics of a hovering helicopter is presented. The results generated from the linear analysis are then compared with the transient and frequency responses measured inflight on the variable-stability

CH-47B research helicopter. A detailed discussion of the parametric effects and a summary of the results of the study completes this report.

2. DYNAMIC INFLOW MODELS

The analysis of the influence of dynamic inflow on helicopter response in the vertical axis focused on two dynamic inflow models related to the thrust of the lifting rotor. The first model was developed by Carpenter and Fridovich in 1953 [13], and the second model was developed by Pitt and Peters [11,12] in 1981. Carpenter extended the simple-momentum theory for steady-state inflow to include the transient inflow buildup by introducing the "apparent additional mass" of air m_a participating in the acceleration. With a steady aircraft vertical velocity w, and accounting for blade flapping, the expression for the instantaneous thrust becomes [13]:

$$T = m_a \dot{v} + 2\pi R^2 \rho v (v - w + (2/3)\dot{\beta} R) \tag{1}$$

By analogy with an accelerating impervious disk, Carpenter defined the apparent additional air mass to be 63.7% of the air mass of the circumscribed sphere of the rotor. Equation (1) thus fits the two end points: at the moment that the inflow transient begins, and at the final steady state. In between, Eq. (1) may not be exact, because the flow fields of the impervious disk and the helicopter rotor are not strictly analogous.

Now expressing (1) in terms of thrust coefficient, and noting that $m_a = 0.637\rho(4/3)\pi R^3$, yields

$$C_T = 0.849 \frac{\dot{\bar{v}}}{\Omega} + 2\bar{v}\left(\bar{v} - \frac{w}{\Omega R} + \frac{2}{3}\frac{\dot{\beta}}{\Omega}\right) \tag{2}$$

where

$$\bar{v} = \frac{v}{\Omega R}$$

Linearizing about the initial conditions, $v = v_o$, $w = w_o$, and $\dot{\beta} = 0$, results in the following perturbation equation:

$$\tilde{C}_T = 0.849\left(\frac{\dot{v}}{\Omega^2 R}\right) + 2\left(2\bar{v}_o - \frac{w_o}{\Omega R}\right)\frac{v}{\Omega R} - 2\bar{v}_o\frac{w}{\Omega R} + \frac{4}{3}\bar{v}_o\frac{\dot{\beta}}{\Omega} \tag{3}$$

The Pitt-Peters dynamic inflow model was developed based on unsteady actuator-disc theory [11,12]. Closed-form formulae were obtained that relate transient rotor thrust and pitch and roll moments to the transient response of the rotor induced-flow field. Applying the Pitt-Peters model in hover, the inflow response to the transient thrust (the nonlinear version with "corrected" value for M_{11}^{12}) is reduced to

$$C_T = \frac{1}{\Omega}\left(\frac{128}{75\pi}\right)\frac{d\bar{v}}{dt} + 2V_T\bar{v} \tag{4}$$

where V_T is the normalized total velocity at the rotor. In order to provide a direct comparison with the Carpenter-Fridovich model above, Eq. (4) is extended to include the effects of the vertical motion of the aircraft and the blade flapping, as follows:

$$C_T = \frac{0.543}{\Omega}\frac{d\bar{v}}{dt} + 2\left(\bar{v} - \frac{w}{\Omega R} + \frac{2}{3}\frac{\dot{\beta}}{\Omega}\right)\bar{v} \tag{5}$$

Equation (5) will henceforth be called the Pitt-Peters model (or the Pitt model for brevity). By comparing Eq. (2) and Eq. (5), it is clear that the two models are now identical with one exception: the Pitt-Peters model

smaller apparent additional air mass by about 64% than does the Carpenter-Fridovich model. Because of the smaller value of m_a associated with the Pitt-Peters model, the time constant of the inflow mode is also smaller as will be discussed in more detail later.

3. EQUATIONS OF MOTION IN HOVER

The small-disturbance equations of motion are obtained by combining the Pitt-Peters dynamic inflow equation described in the preceding section with the flapping equation [14,15], and the vertical motion of the helicopter. The results are shown in Table 1 for an articulated rotor with no hinge offset or pitch-flap coupling. The fuselage drag and the effects of rotor downwash on the fuselage are neglected. In these equations, the value of the constant C_o is 1 for the Pitt-Peters dynamic inflow model, and is 0.639 for the Carpenter-Fridovich model. It can readily be verified, in fact, that the set of equations in Table 1 is identical to that of the linearized version of the set of nonlinear equations developed in Ref. [13], if the rotor RPM is assumed to remain constant.

To provide some background for the results to be discussed in the subsequent sections, it is important at this point to examine two special cases: (1) the quasi-static equation, and (2) hover equations with no aircraft motions.

3.1 *Quasi-Static Equation*

The classical quasi-static equation for the uncoupled vertical motion of the helicopter can now be reduced from the general equations in Table 1 by assuming that the inflow and the flapping reach their steady state instantaneously upon an input in collective pitch. Setting the time rate of change in

inflow, the flapping rate, and flapping acceleration to zero, the fourth-order equation in Table 1 reduces to the following first order equation:

$$\dot{w} = Z_w w + Z_\theta \theta \tag{6}$$

where

$$Z_w = - \frac{\rho a \sigma (\Omega R)}{8(m/\pi R^2)(1 + a\sigma/16\bar{\nu}_o)} \tag{7}$$

$$Z_\theta = - \frac{4}{3} \Omega R Z_w \tag{8}$$

As expected, the quasi-static equation shown above does not contain the parameter C_o and is, therefore, independent of the dynamic inflow model used. Note also that the quasi-static derivatives Z_w and Z_θ are independent of the mass and inertia properties of the rotor blade. These derivatives vary significantly with flight conditions such as air density, thrust coefficient, and disc loading. The quasi-static derivative Z_w (commonly called vertical damping) as expressed in Eq. (7) is in good agreement with the approximation given by Seckel in Ref. [17].

3.2 *Hover Equation with No Aircraft Motion*

To compare the predicted response with Carpenter-Fridovich's experimental data from a hover-test tower, it is instructive to examine the case wherein the aircraft motion is absent. With the vertical motion neglected, the coupled inflow and flapping equations become:

$$\frac{d}{dt}\begin{Bmatrix} v \\ \beta \\ \dot{\beta} \end{Bmatrix} = \begin{bmatrix} -\frac{75\pi\Omega}{32}\left(\bar{\nu}_o + \frac{a\sigma}{16}\right)C_o & 0 & -\frac{25\pi\Omega R}{32}\left(\bar{\nu}_o + \frac{a\sigma}{8}\right)C_o \\ 0 & 0 & 1 \\ -\frac{\Omega\gamma}{6R} & -\Omega^2 & -\frac{\Omega\gamma}{8} \end{bmatrix} \begin{Bmatrix} v \\ \beta \\ \dot{\beta} \end{Bmatrix}$$

$$+ \begin{bmatrix} \frac{25\pi\Omega^2 R}{32}\left(\frac{a\sigma}{8}\right)C_o \\ 0 \\ \frac{\Omega^2\gamma}{8} \end{bmatrix} \theta_o \qquad (9)$$

From this set of equations, several versions of reduced forms are given in Table 2, including the "quasi-steady inflow" approximation [16], which, in effect, assumes that the apparent additional mass is zero. It is clear from this table, that for the quasi-steady inflow approximation there exists no equivalent Lock number that accounts for the vertical inflow effect in the flapping equation. This result is in contrast to the work of Curtiss and Shupe [16], in which they discovered that there is an equivalent Lock number associated with the pitch-and-roll motion of the helicopter when the quasi-steady inflow approximation is used in the first harmonic inflow variation.

The steady-state responses of the inflow and flapping to a step input in collective pitch can be obtained from Eq. (9) as:

$$(v/\theta_o)_{s.s.} = \frac{a\sigma(\Omega R)}{24[\bar{\nu}_o + a\sigma/16]} \tag{10}$$

$$(\beta/\theta_o)_{s.s.} = \frac{\gamma}{8}\frac{\bar{\nu}_o + a\sigma/144}{\bar{\nu}_o + a\sigma/16} \tag{11}$$

which indicate that the change in inflow is purely aerodynamic in nature. However, the change in the flapping depends on the operating conditions and the inertia properties of the rotor blade. An inspection of these equations reveals that the steady-state sensitivities of inflow and flapping with respect to collective pitch vary widely with operating condition, going from $(2/3)\Omega R$ and $\gamma/72$ at $\bar{\nu}_o = 0$ (zero initial thrust condition), to $(a\sigma/24\bar{\nu}_o)\Omega R$ and $\gamma/8$ as $\bar{\nu}_o >> a\sigma/16$. The extremely large variations in the response characteristics with operating condition indicate that the system is highly nonlinear. Thus, care must be exercised in interpreting the results obtained using the linearized equations of motion when calculating the responses of inflow, flapping, and thrust to a large collective pitch input.

4. COUPLED INFLOW-FLAPPING DYNAMICS

The hover equation with no aircraft motion will first be examined in some detail to determine how the coupled inflow-flap dynamics are influenced by the dynamic inflow model used. The effects of the rotor-operating conditions (in terms of thrust coefficient) and the Lock number of the rotor blade are also investigated, with the focus on their influence on the flapping and thrust overshoot characteristics. For correlation with the flight-test data of the CH-47B helicopter to be presented later in the discussion of the case with aircraft motion, a rotor-system similar to the CH-47B will be used in the

following calculations. The rotor rotational speed, solidity ratio, and the tip speed are 24.085 r/s, 0.067, and 722.55 ft/s, respectively.

4.1 *Influence of Lock Number*

Although the uncoupled inflow dynamics are independent of the rotor blade inertia, the inflow mode in the coupled inflow-flap dynamics is strongly influenced by the blade Lock number as shown in Fig. 1. For an operating condition with a moderate level of thrust coefficient (C_T = 0.0047), the time constant of the inflow mode corresponding to the lower values of Lock number (γ = 3-6) is on the order of 1/10 sec for the Carpenter-Fridovich dynamic inflow model, and on the order of 1/16 sec for the Pitt-Peters inflow model. For both inflow models, the time constant of the inflow mode reduces rapidly as the Lock number increases. Both inflow models have a strong effect on the frequency and damping of the flapping mode as is evident by comparing them with the case of no inflow dynamics shown in Fig. 1. Notice that, with both dynamic inflow models, the frequency and damping of the flapping mode are reduced from the uncoupled flapping mode (without dynamic inflow) for the entire range of Lock number. Compared with Carpenter's model, Pitt's model produces a more destabilizing influence on the flapping mode.

The transient characteristics of the inflow and flapping responses to a step input in collective pitch (0.01 rad) are shown in Fig. 2 for a low value (γ = 3) and a high value (γ = 16) of the blade Lock number for both dynamic inflow models. The more destabilizing effect of Pitt's model is evident. The inflow response, while monotonically increasing for the low value of the blade Lock number (and at the moderate value of thrust coefficient C_T = 0.0047), tends to oscillate initially before reaching its steady-state value for the high value of the blade Lock number. The steady-state values of the inflow

and flapping responses are independent of the dynamic inflow model used as discussed earlier. As expected from Fig. 1, the responses for the low value of the blade Lock number are more oscillatory and the overshoot in flapping (and, thus, thrust) higher than those for the high value of the blade Lock number.

Figure 3 shows the influence of the blade Lock number on the overshoot of the flapping response to a step input in collective pitch at the moderate value of thrust coefficient (C_T = 0.0047). The percent overshoot increases greatly with decreasing Lock number for both the dynamic inflow models, with Carpenter's model producing slightly larger overshoot than does Pitt's. Both models induce a larger flapping overshoot than exists without including a dynamic inflow model, for the entire range of blade Lock number examined. Figure 4 shows a comparison of flapping and thrust responses of the two cases; one with Carpenter's dynamic inflow model, and the other including no dynamic inflow, for γ = 8.608 and C_T = 0.0047.

4.2 *Effect of Thrust Coefficient*

As discussed earlier, the initial thrust coefficient has a strong effect on the steady-state responses of inflow and flapping to collective input. Its influence on the coupled inflow-flap dynamic modes is also very strong as shown in Fig. 5. For γ = 8.608, the inflow mode has a time constant of 1/3 sec for Carpenter's model (about 1/5 sec for the Pitt's) at C_T = 0. The inflow mode time constant decreases rapidly with increasing thrust coefficient for both dynamic inflow models. Both models induce a lower frequency of the flapping mode, comparing with the case of no dynamic inflow as shown in the figure.

Figure 6 shows the flapping and inflow responses to step input in collective pitch for a low value (C_T = 0.00135) and a high value (C_T = 0.008) of thrust coefficient. The steady-state response of the blade flapping has a higher value, and the inflow response a lower value, for higher initial thrust coefficient. Again, the Pitt's dynamic inflow model induces a more oscillatory response than does Carpenter's model. For a low value of initial C_T (and with a moderate value of the blade Lock number, γ = 8.608 in this case), the inflow response is monotonically increasing; however, it is oscillatory initially for the larger value of C_T, an effect similar to that of increasing Lock number discussed earlier. The inflow and the flapping responses reach their steady values less than 1 sec following the step input in collective. The influence of thrust coefficient on the flapping (and, thus, thrust) overshoot is also very strong as indicated in Fig. 7. The flapping overshoot increases with decreasing thrust coefficient more rapidly in the low-thrust region. Again, Carpenter's model produces slightly more overshoot than does Pitt's.

In summary, when the aircraft vertical motion is restricted such as when performing a test on a hover test stand, the inflow and the flapping reach their steady state within 1 sec or less following an abrupt input in collective pitch (as previously shown in Ref. [13]). However, the shape of the inflow response and the overshoot in flapping and thrust responses are dependent strongly upon the blade Lock number and the thrust coefficient. In particular, the overshoot in flapping and thrust responses increases with a decrease in Lock number or in thrust coefficient. The percent overshoot can deviate considerably from about 100% as predicted in Ref. [13], especially with a larger value of blade Lock number or at a higher level of thrust coefficient or both.

5. VERTICAL RESPONSE OF THE HELICOPTER IN HOVER

The coupled inflow-flapping-vertical motion of the helicopter is now examined using the equations of motion listed in Table 1. The rotational speed of the rotor is assumed to be constant. Before proceeding with the determination of the influence of operating conditions and the blade inertia characteristics as was done in the preceding section, the calculated vertical acceleration response from the Table 1 model will be compared with that measured from flight using a CH-47 research aircraft [18]. Comparison will be made for both the step response and the frequency response characteristics to collective pitch excitation.

5.1 *Comparison of Transient Response with the CH-47 Test Data*

The normal acceleration response to a sequence of 15 sec pulse inputs in collective was measured on the CH-47 as shown in Fig. 8. The amplitude of the collective pulse is approximately 0.62 in. (0.0201 rad). The data were taken initially with a sampling frequency of 107.75 Hz. They were then passed through a filter with a response flat up to 5 Hz and cutting off by more than 44 dB above 6.5 Hz [19] to remove the 3/rev and higher harmonic vibratory noise. Finally, the filtered data were decimated by a factor of 5 to yield 21.55 Hz data, as plotted in Fig. 9. As can be seen, the transient is characterized by an overshoot in a_z which immediately follows an abrupt change in collective pitch. The response of the rotor RPM was not recorded, but some small variations in rotor RPM, on the order of 3%, were observed from a video recording of the cockpit instrumentation during the flight. The response of the RPM is slower than that of a_z, typically drooping down to its minimum at about 1 sec after an up collective, and the transient lasts for about 3 sec before reaching steady state.

The calculated perturbation of the vertical acceleration response to a 0.62 in. step input in collective pitch is shown in Fig. 10 with both dynamic inflow models. The first peak of the calculated a_z response is about 9.9 ft/sec^2 which is somewhat smaller than the measured value of about 11 ft/sec^2, and the calculated value at $t = 5$ sec is somewhat larger than that measured. The second peak of the calculated response, because of the constant RPM assumption used in the math model, tends to be sharper than the measured, especially with Pitt's inflow model. As in the case with no aircraft motion, Pitt's dynamic inflow model tends to produce more oscillatory response in a_z than does the Carpenter model.

An inspection of the a_z response shown in Fig. 10 reveals that there is a small initial undershoot of about 1.9 ft/sec^2. This is due to the assumption that the rotor blade is rigid (infinite blade-bending stiffness), which results in overly large inertia forces, as previously observed by Carpenter [13]. This effect may be incorporated into the equations of motion in Table 1 by selecting the reduced mass moment M_β so that the initial undershoot will be zero. If M_β is chosen to be

$$M_\beta = \frac{4I_\beta}{3R} \tag{12}$$

then, the forcing function in the acceleration equation becomes zero, resulting in a no-undershoot response as shown in Fig. 11. (It is interesting to note that the above expression for M_β amounts to a reduction of approximately 11% from the value corresponding to a rectangular blade with a uniform mass distribution, i.e., $M_\beta = 3I_\beta/2R$.) Also shown in the figure is the calculated a_z response with no dynamic inflow (constant inflow). The strong

influence of the dynamic inflow on the overshoot in the vertical acceleration response is clearly exhibited in the figure.

5.2 *Comparison of Frequency Response*

A varying frequency input in collective pitch was employed to measure the frequency response of a_z to collective of the CH-47B research aircraft. Figure 12 shows a sample of typical frequency sweeps, with frequency varying from about 0.05 Hz to about 2 Hz. Using the Fourier analysis programs developed in Ref. [20], the frequency response of a_z/δ_c was determined as shown in Fig. 13. From the amplitude plot, it is seen that there is a resonance peak at the frequency of about 17 rad/sec. It is also interesting to note from the phase plot, that a substantial lead is present in the range of frequencies below 6.5 rad/sec. Because of lack of low-frequency power in the frequency sweeps (see Fig. 11), the identified frequency-response plots become less reliable in the range of frequencies below 0.3 rad/sec.

The calculated frequency response of the a_z/δ_c transfer function using the math model listed in Table 1 is shown in Fig. 14, with the flight data, for both Carpenter's and Pitt's dynamic inflow models. The calculations cover the frequency range of 0.1 to 100 rad/sec. The resonance peak at the frequency of about 17 rad/sec is evident, with Pitt's model producing a slightly higher peak than Carpenter's because of the more destabilized flapping mode. (A more detailed discussion will be given later.) The low-frequency phase lead observed in the flight-measured phase plot is also seen in the calculated phase plots for both inflow models. This phase lead is a result of the non-minimum phase behavior of the a_z/δ_c transfer function and a free s present in the numerator. Overall, the frequency responses calculated with the two

dynamic inflow models match well with those measured from flight test using the CH-47B research helicopter. It should be noted that the intent here is not to provide a direct correlation, since the simplified math model was developed for a single-main rotor helicopter with constant RPM, and without accounting for rotor to rotor interference effects as will be present in the CH-47B tandem-rotor helicopter.

5.3 *Influence of Lock Number*

We now examine the influence of Lock number on the coupled inflow-flap-body vertical dynamics. First, the effect of aircraft motion on the inflow and the flapping modes is determined by comparing directly their eigenvalues as shown in Fig. 15. Clearly, both the inflow mode and the flapping mode are relatively insensitive to the vertical motion of the helicopter. With the vertical motion, the heave mode is insensitive to the variation in the blade Lock number and to the dynamic inflow model used. The eigenvalue of the heave mode is on the order of -0.29 1/sec, and since it is well separated frequency-wise from the inflow and flapping modes, the heave mode eigenvalue can be adequately approximated by the quasi-static Z_w as given in Eq. (6).

The effect of the blade Lock number on the vertical acceleration, and the rate of climb responses to a step input in collective pitch (0.01 rad) is shown in Fig. 16. Pitt's dynamic inflow model is used in the computation because it is, in general, more oscillatory as discussed previously. The lower value of Lock number yields a more oscillatory response than does the higher value, as is to be expected from Fig. 15. Because of the high-order dynamic effects, there is a retardation (on the order of 50 ms) in the rate of climb response. Thus, the delay effect may have to be considered, if the

simple quasi-static equation (6) is used in the design analysis of a highly augmented vertical axis.

5.4 *Influence of Thrust Coefficient*

With the aircraft motion included, the thrust coefficient was varied by changing the weight of the aircraft. The effect of changing the thrust coefficient on the system eigenvalues is shown in Fig. 17. While the flapping mode is relatively insensitive with respect to the variation in the thrust coefficient, both the inflow and the heave modes are significantly affected. The time constant of the inflow mode is reduced as the thrust coefficient is increased, as is the case without aircraft motion discussed previously; the heave-mode time constant is decreased with increasing thrust coefficient. The heave mode is relatively insensitive to the dynamic inflow model used as can be expected from the expression (7) for the quasi-static vertical damping. However, it is evident that both the inflow and the flapping modes are significantly influenced by the dynamic model used. With the Pitt model, which in effect reduces the additional apparent air mass relative to the Carpenter model, there is a decrease in the inflow-mode time constant and a destabilizing effect on the flapping mode. Reducing further the additional apparent air mass to zero yields, in the limit, the quasi-static inflow [16]. For this limiting case, the time constant of the inflow mode becomes zero and the flapping mode is further destabilized from that corresponding to the Pitt's model as shown in Fig. 17.

As in the case with no aircraft motion, a decrease in the thrust coefficient also results in an increased thrust overshoot in response to a rapid collective input when the aircraft vertical motion is included. This effect is shown in Fig. 18, in which a low and a high value of thrust coefficient are

compared. Note, also, from the figure that the effective time constant of the a_z decaying response following the initial transient decreases with the decreased thrust coefficient owing to an increase in the quasi-static vertical damping Zw as discussed earlier. This decrease in the effective time constant is also apparent in the heave response. Notice that the initial delay in the heave response is again evident in the figure. The calculations using Carpenter's dynamic inflow model result in less oscillatory responses comparing to those shown in Fig. 18 because of the more stable predicted flapping mode exhibited in Fig. 17.

6. CONCLUDING REMARKS

This paper has described a study conducted to gain a better understanding of the influences of dynamic inflow on the vertical motion of the helicopter. Two dynamic inflow models, one by Carpenter-Fridovich developed in 1953, and one by Pitt-Peters developed in 1981, were investigated in conjunction with variations in thrust coefficient and the rotor blade Lock number. Linearized versions of these models were developed for use in the design analysis of high-bandwidth control systems for rotorcraft, and to gain a better insight into the interplay of the dynamic inflow, rotor blade flapping, and the vertical motion of the rotorcraft. Comparisons of these analytic models were made with flight test results of the NASA Ames CH-47B helicopter. The results of the study are summarized in the following:

1. Generally, good agreement was obtained between both the transient and frequency responses generated from the linear model and those measured from the CH-47B research helicopter. For the transient response to a step input in collective input, the model well predicts the initial vertical acceleration overshoot and its long-term decaying rate. However, the agreement in mid-term

response is degraded somewhat due perhaps to the constant RPM assumption used in the linear model.

2. Dynamic inflow plays a key role in the initial overshoot of the vertical acceleration response to an abrupt input in the collective. It destabilizes the flapping (coning) mode, and it introduces a new inflow mode. The overshoot in the vertical acceleration response becomes more pronounced as the thrust coefficient is decreased or the rotor blade Lock number is lowered or both. The time constant of the inflow mode decreases with an increase in Lock number or an increase in the value of thrust coefficient. The time constant of the body-heave mode increases with increasing thrust coefficient and is insensitive to the variation in Lock number. Neither the flapping mode nor the inflow mode is significantly affected by the vertical motion of the helicopter.

3. Compared with Carpenter's dynamic inflow model, Pitt's model tends to produce more oscillatory responses owing to its more destabilizing influence on the flapping mode. The time constant of the inflow mode is smaller for Pitt's model than for Carpenter's, because Pitt's model, in effect, reduces the additional apparent air mass participating in the inflow transient from that of Carpenter's. A further reduction in the additional apparent air mass to zero yields the quasi-static inflow for which the time constant of the inflow mode is zero.

4. Because of the high-order effect owing to the inflow and flapping modes, there is a retardation on the order of 50 ms in the response of vertical rate of climb for the rotor system evaluated.

5. The transfer function of the vertical acceleration to collective has a nonminimum phase characteristic, which together with a free s present in

the numerator results in a significant phase lead in the frequency range below approximately 6.5 rad/s.

REFERENCES

1. McRuer, D., Johnson, D., and Meyers, T., A perspective on speraugmented flight control advantages and problems. AGARD Conference on Active Control, Ontario, Canada (1984).
2. Landis, K. H. and Glusman, S. I., Development of ADOCS controllers and control laws. Vol. I to III, NASA CR 177339, (March 1985).
3. Chen, R. T. N. and Hindson, W. S., Influence of high-order dynamics on helicopter flight control system bandwidth. AIAA J. Guidance, Control, and Dynamics, 9, No. 2, 190-197 (1986).
4. Hilbert, K. B., Lebacqz, J. V., and Hindson, W. S., Flight investigation of a multivariable model-following control system for rotorcraft. AIAA Paper 86-9779, AIAA 3rd Flight Test Conf., Las Vegas, Nevada, (April 2-4, 1986).
5. Miller, R. H., A method for improving the inherent stability and control characteristics of helicopters. J. Aero. Sci., 363-374, (June 1950).
6. Ellis, W. C., Effects of articulated rotor dynamics on helicopter automatic control system requirements. Aero. Eng. R., 30-38, (July 1953).
7. Hall, W. E., Jr. and Bryson, A. E., Jr., Inclusion of rotor dynamics in controller design. J. Aircraft, Vol. 10, 100-206, (April 1973).
8. Ormiston, R. A., Application of simplified inflow models to rotorcraft dynamic analysis. J. Am. Helicopter Sci., 34-37, (July 1976).
9. Johnson, W., Influence of unsteady aerodynamics on hingeless rotor ground resonance. J. Aircraft 19, 668-673 (1982).
10. Friedmann, P. P. and Venkatesan, C., Influence of various unsteady aerodynamic models on the aeromechanical stability of a helicopter in ground resonance. NASA CP-2400, 207-218 (1985).

11. Gaonkar, G. H. and Peters, D., A review of dynamic inflow and its effect on experimental correlations. NASA CP-2400, 187-203 (1985).

12. Pitt, D. M. and Peters, D. A., Theoretical prediction of dynamic-inflow derivatives. Vertica 5, 21-34 (1981).

13. Carpenter, P. J. and Fridovich, B., Effect of a rapid-pitch increase on the thrust and induced-velocity response of a full-scale helicopter rotor. NACA TN-3044 (1953).

14. Chen, R. T. N., A simplified rotor system mathematical model for piloted flight dynamics simulation. NASA TM-78575 (1979).

15. Chen, R. T. N., Effects of primary rotor parameters on flapping dynamics. NASA TP-1431 (1980).

16. Curtiss, H. C., Jr. and Shupe, N. K., A stability and control theory for hingeless rotors. AHS National Forum Preprint No. 541 (1971).

17. Seckel, E., Stability and control of airplanes and helicopters. Academic Press, New York and London (1964).

18. Hindson, W. S., Hilbert, K. B., Tucker, G. E., Chen, R. T. N., and Fry, E. B., New capabilities and recent research programs of the NASA/Army CH-47B variable-stability helicopter. Presented at the 42nd AHS National Forum, Washington, D.C. (1986).

19. Milne, G., Interim report for a doctoral thesis. Identification of a high bandwidth hover control model for the CH-47B helicopter. Stanford University (1986).

20. Tischler, M. B., Leung, J. G. M., and Dugan, D. C., Frequency-domain identification of XV-15 tilt-rotor/aircraft dynamics. J. Am. Helicopter Soc. 30, No. 2 (1985).

Table 1. Equations of Motion

$$\frac{d}{dt}\begin{Bmatrix} v \\ \beta \\ \dot{\beta} \\ w \end{Bmatrix} = \begin{bmatrix} -\frac{75\pi\Omega}{32}\left(\bar{\nu}_0 - \frac{W_0}{2\Omega R} + \frac{a\sigma}{16}\right)C_0 & 0 & -\frac{25\pi\Omega R}{32}\left(\bar{\nu}_0 + \frac{a\sigma}{8}\right)C_0 & \frac{75\pi\Omega}{64}\left(\bar{\nu}_0 + \frac{a\sigma}{8}\right)C_0 \\ 0 & 0 & 1 & 0 \\ -\frac{\Omega\gamma}{\Delta R}\left(\frac{1}{6} - \frac{NM_\beta}{4mR}\right) & -\frac{\Omega^2}{\Delta} & -\frac{\Omega\gamma}{\Delta}\left(\frac{1}{8} - \frac{NM_\beta}{6mR}\right) & \frac{\Omega\gamma}{\Delta R}\left(\frac{1}{6} - \frac{NM_\beta}{4mR}\right) \\ \frac{N\Omega\gamma}{\Delta Rm}\left(\frac{I_\beta}{4R} - \frac{M_\beta}{6}\right) & -\frac{NM_\beta\Omega^2}{m\Delta} & \frac{N\Omega\gamma}{\Delta m}\left(\frac{I_\beta}{6R} - \frac{M_\beta}{8}\right) & -\frac{N\Omega\gamma}{\Delta mR}\left(\frac{I_\beta}{4R} - \frac{M_\beta}{6}\right) \end{bmatrix} \begin{Bmatrix} v \\ \beta \\ \dot{\beta} \\ w \end{Bmatrix}$$

$$+ \begin{bmatrix} \frac{25\pi\Omega^2 Ra\sigma}{256} C_0 \\ 0 \\ \frac{\Omega^2\gamma}{\Delta}\left(\frac{1}{8} - \frac{NM_\beta}{6mR}\right) \\ -\frac{N\Omega^2\gamma}{\Delta m}\left(\frac{I_\beta}{6R} - \frac{M_\beta}{8}\right) \end{bmatrix} \theta_0$$

where

$$\Delta = 1 - \frac{NM_\beta^2}{mI_\beta}$$

$$\gamma = \frac{\rho acR^4}{I_\beta}$$

$$\bar{\nu}_0 = \sqrt{\frac{C_{T_0}}{2}}$$

Table 2. Several Versions of Equations of Motion (without including aircraft motion)

I. With dynamic inflow

$$\frac{d}{dt}\begin{Bmatrix} v \\ \beta \\ \dot{\beta} \end{Bmatrix} = \begin{bmatrix} -\frac{75\pi\Omega}{32}\left(\bar{\nu}_0 + \frac{a\sigma}{16}\right)C_0 & 0 & -\frac{25\pi\Omega R}{32}\left(\bar{\nu}_0 + \frac{a\sigma}{8}\right)C_0 \\ 0 & 0 & 1 \\ -\frac{\Omega\gamma}{6R} & -\Omega^2 & -\frac{\Omega\gamma}{8} \end{bmatrix} \begin{Bmatrix} v \\ \beta \\ \dot{\beta} \end{Bmatrix} + \begin{bmatrix} \frac{25\pi\Omega^2 R}{32}\left(\frac{a\sigma}{8}\right)C_0 \\ 0 \\ \frac{\Omega^2\gamma}{8} \end{bmatrix} \theta_0$$

II. Quasi-steady inflow ($\dot{\bar{\nu}} = 0$)

$$\frac{d}{dt}\begin{Bmatrix} \beta \\ \dot{\beta} \end{Bmatrix} = \begin{bmatrix} 0 & 1 \\ -\Omega^2 & -\frac{\Omega\gamma}{8}\left(1 - \frac{8\bar{\nu}_0 + a\sigma}{18(\bar{\nu}_0 + a\sigma/16)}\right) \end{bmatrix} \begin{Bmatrix} \beta \\ \dot{\beta} \end{Bmatrix} + \begin{bmatrix} 0 \\ \frac{\Omega^2\gamma}{8}\left(1 - \frac{a\sigma}{18(\bar{\nu}_0 + a\sigma/16)}\right) \end{bmatrix} \theta_0$$

III. Steady inflow (ν = const.)

$$\frac{d}{dt}\begin{Bmatrix} \beta \\ \dot{\beta} \end{Bmatrix} = \begin{bmatrix} 0 & 1 \\ -\Omega^2 & -\frac{\Omega\gamma}{8} \end{bmatrix} \begin{Bmatrix} \beta \\ \dot{\beta} \end{Bmatrix} + \begin{bmatrix} 0 \\ \frac{\Omega^2\gamma}{8} \end{bmatrix} \theta_0^* \qquad \theta_0^* = \theta_0\left[1 - \frac{a\sigma}{18(\bar{\nu}_0 + a\sigma/16)}\right]$$

IV. No inflow changes

$$\frac{d}{dt}\begin{Bmatrix} \beta \\ \dot{\beta} \end{Bmatrix} = \begin{bmatrix} 0 & 1 \\ -\Omega^2 & -\frac{\Omega\gamma}{8} \end{bmatrix} \begin{Bmatrix} \beta \\ \dot{\beta} \end{Bmatrix} + \begin{bmatrix} 0 \\ \frac{\Omega^2\gamma}{8} \end{bmatrix} \theta_0$$

Figure Captions

Fig. 1: Influence of blade Lock number on characteristic roots (without A/C motion).

Fig. 2: Effect of Lock number on inflow and flapping responses to collective input (Ω = 24.085 r/s, σ = 0.067, ΩR = 722.55 ft/s, C_T = 0.0047, collective step = 0.01 rad). (a) Carpenter inflow model, (b) Pitt inflow model.

Fig. 3: Influence of Lock number on flapping overshoot.

Fig. 4: Effect of dynamic inflow on flapping and thrust response (γ = 8.608, Ω = 24.085 r/s, σ = 0.067, ΩR = 722.55 ft/s, collective step = 0.01 rad. C_T = 0.0047).

Fig. 5: Effect of thrust coefficient on characteristic roots.

Fig. 6: Effect of thrust coefficient on inflow and flapping responses to collective input (γ = 8.608, Ω = 24.085 r/s, σ = 0.067, ΩR = 722.55 ft/s, collective step = 0.01 rad). (a) Carpenter inflow model, (b) Pitt inflow model.

Fig. 7: Influence of thrust coefficient on flapping overshoot to step input in collective pitch.

Fig. 8: Collective input and a_z response measured on the CH-47B.

Fig. 9: Filtered a_z response: (a) unexpanded scale, (b) expanded scale.

Fig. 10: Calculated perturbed vertical acceleration response to 0.62 in. step collective input: (a) with Carpenter model, (b) with Pitt model.

Fig. 11: Calculated perturbed vertical acceleration response to 0.62 in. step collective input: (a) with carpenter model, (b) Pitt model, (c) no dynamic inflow.

Fig. 12: Frequency sweeps of collective and a_z response measured on the CH-47B.

Fig. 13: Measured frequency response of a_z/δ_c (ft/sec^2/in.) for the CH-47B.

Fig. 14: Calculated frequency response of a_z/δ_c (ft/sec^2/in.) compared with flight data: (a) Carpenter inflow model, (b) Pitt inflow model.

Fig. 15: Influence of blade Lock number on characteristic roots (with and without A/C motion).

Fig. 16: Influence of Lock number on the vertical acceleration and rate of climb responses to collective step input (0.01 rad) (Ω = 24.085 r/s, ΩR = 722.55 ft/s, σ = 0.067, C_T = 0.0047, Pitt inflow model).

Fig. 17: Effect of thrust coefficient on characteristic roots (with A/C vertical motion).

Fig. 18: Influence of thrust coefficient on the vertical acceleration and rate of climb responses to collective step input (0.01 rad) (Ω = 24.085 r/s, ΩR = 722.55 ft/s, σ = 0.067, γ = 8.608, Pitt inflow model).

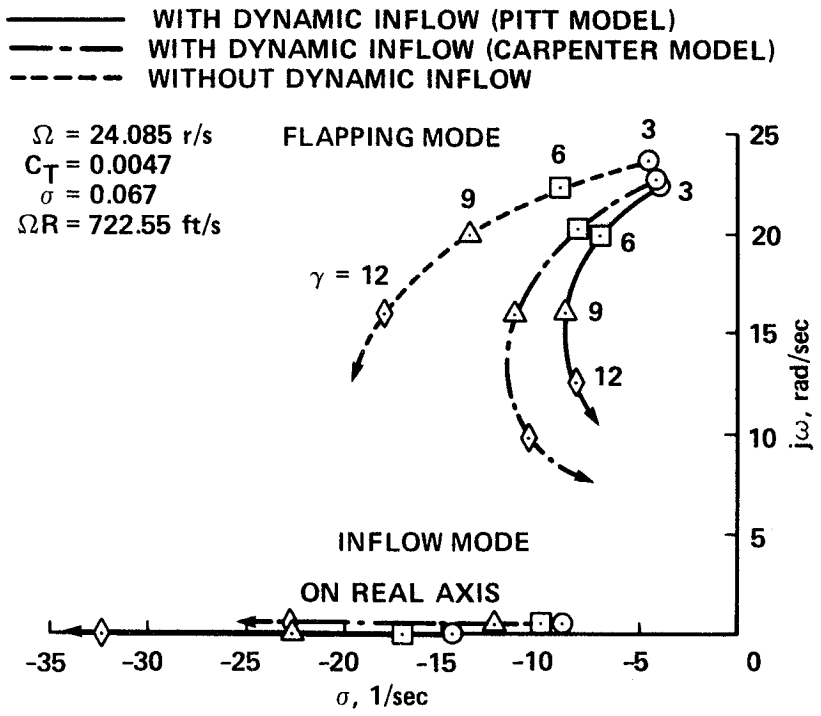
WITH DYNAMIC INFLOW (PITT MODEL)
WITH DYNAMIC INFLOW (CARPENTER MODEL)
WITHOUT DYNAMIC INFLOW
Ω = 24.085 r/s
C_T = 0.0047
σ = 0.067
ΩR = 722.55 ft/s
FLAPPING MODE
INFLOW MODE
ON REAL AXIS
γ = 12
3
6
9
12
25
20
15
10
5
jω, rad/sec
-35
-30
-25
-20
-15
-10
-5
0
σ, 1/sec

Fig. 1

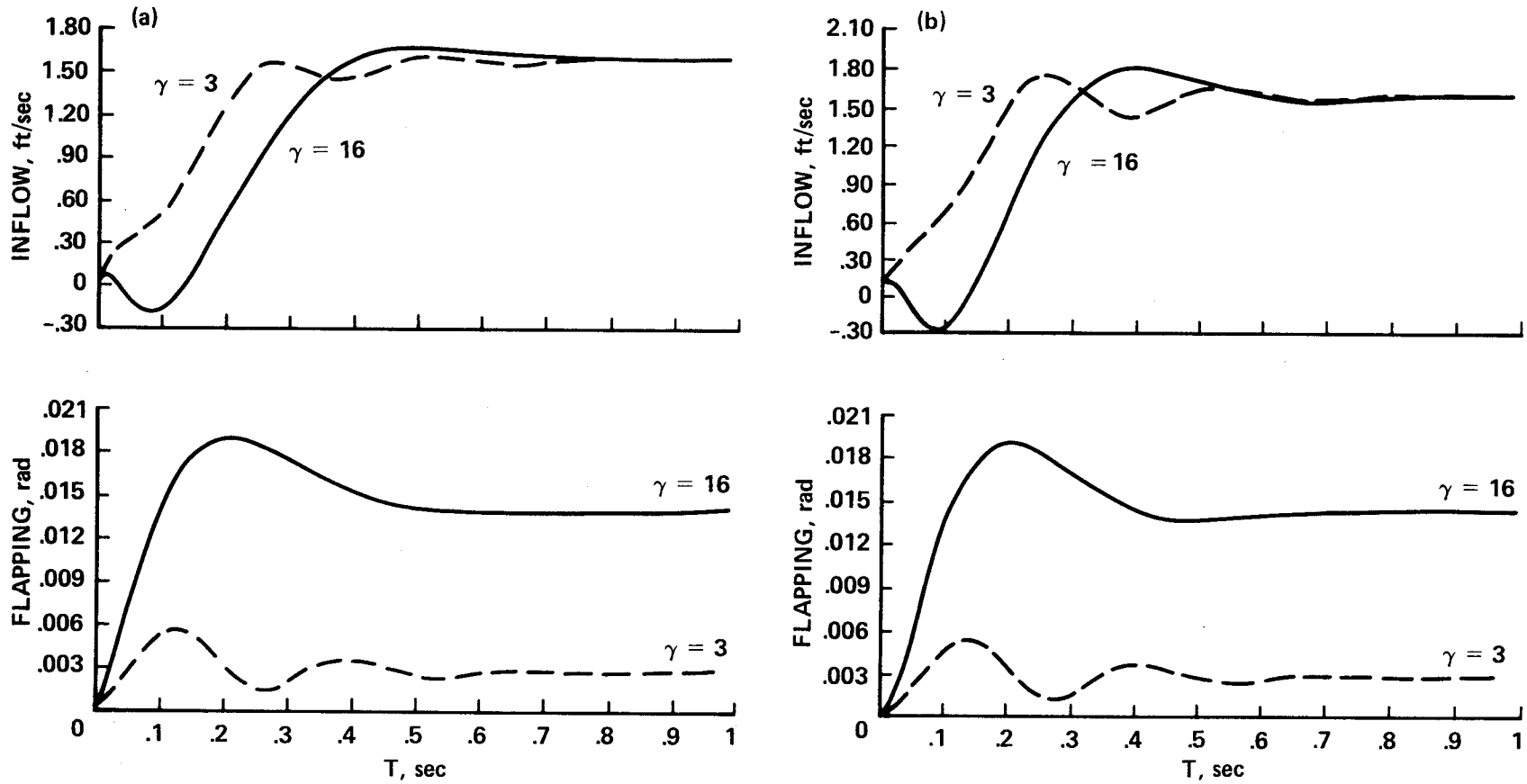
(a)
INFLOW, ft/sec
1.80
1.50
1.20
.90
.60
.30
0
-.30
γ = 3
γ = 16
FLAPPING, rad
.021
.018
.015
.012
.009
.006
.003
0
.1
.2
.3
.4
.5
.6
.7
.8
.9
1
T, sec
γ = 16
γ = 3
(b)
INFLOW, ft/sec
2.10
1.80
1.50
1.20
.90
.60
.30
0
-.30
γ = 3
γ = 16
FLAPPING, rad
.021
.018
.015
.012
.009
.006
.003
0
.1
.2
.3
.4
.5
.6
.7
.8
.9
1
T, sec
γ = 16
γ = 3

Fig. 2

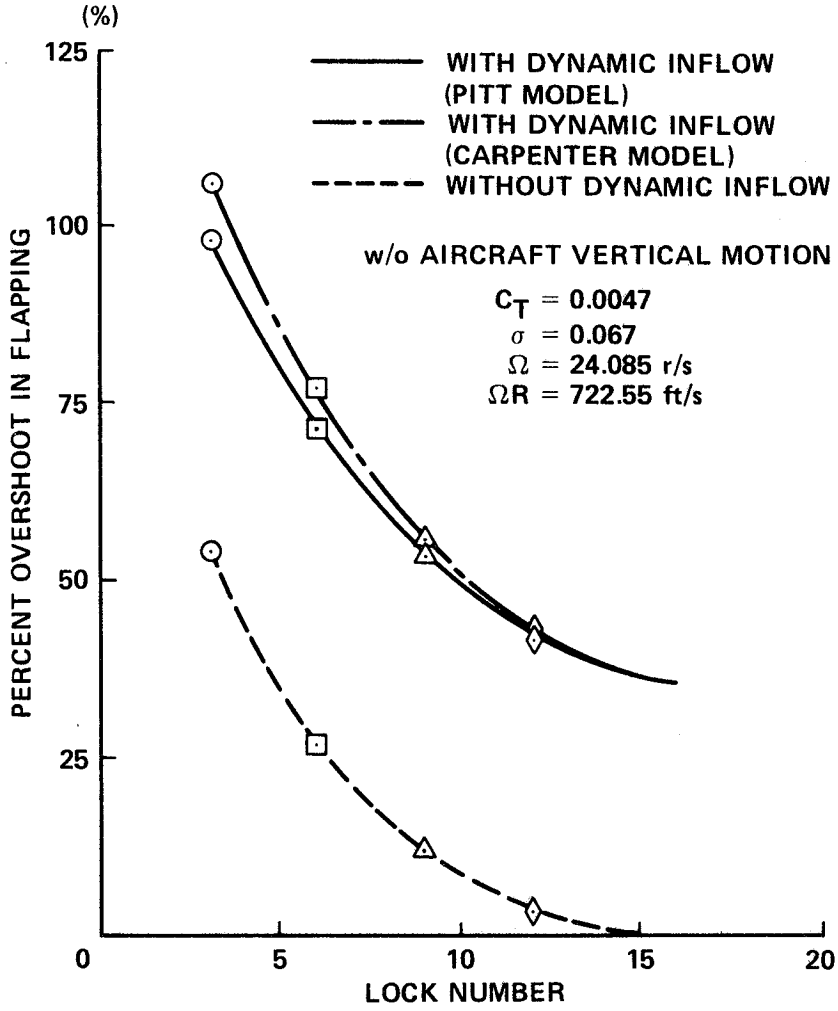
(%)
125
100
75
50
25
0
5
10
15
20
PERCENT OVERSHOOT IN FLAPPING
LOCK NUMBER
WITH DYNAMIC INFLOW (PITT MODEL)
WITH DYNAMIC INFLOW (CARPENTER MODEL)
WITHOUT DYNAMIC INFLOW
w/o AIRCRAFT VERTICAL MOTION
C_T = 0.0047
σ = 0.067
Ω = 24.085 r/s
ΩR = 722.55 ft/s

Fig. 3

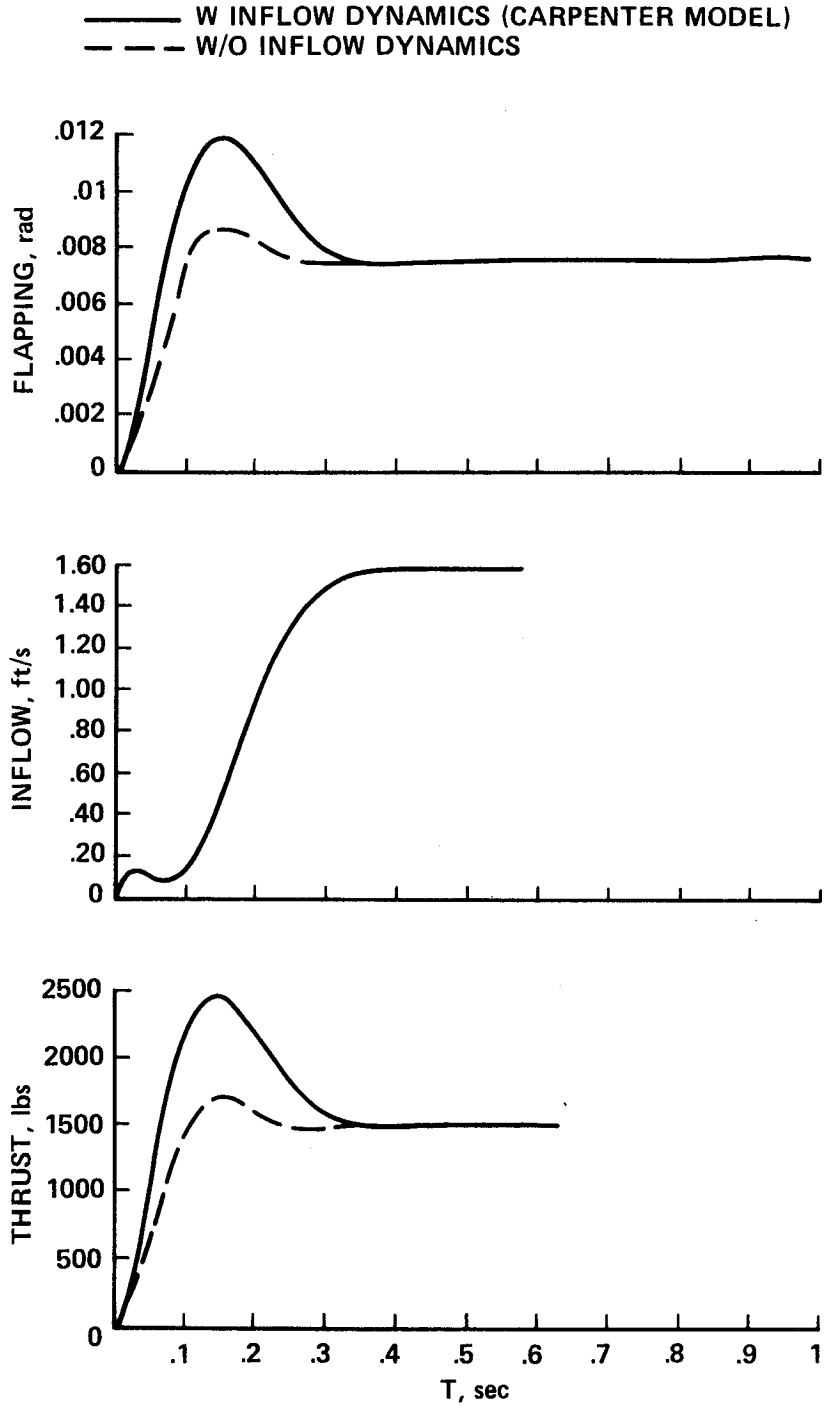
W INFLOW DYNAMICS (CARPENTER MODEL)
W/O INFLOW DYNAMICS
FLAPPING, rad
.012
.01
.008
.006
.004
.002
0
INFLOW, ft/s
1.60
1.40
1.20
1.00
.80
.60
.40
.20
0
THRUST, lbs
2500
2000
1500
1000
500
0
.1
.2
.3
.4
.5
.6
.7
.8
.9
1
T, sec

Fig. 4

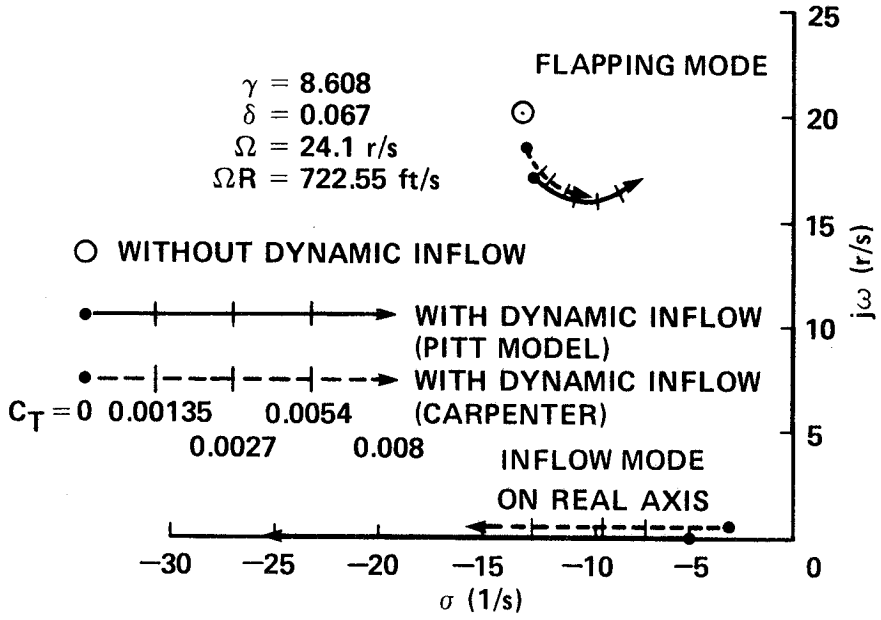
γ = 8.608
δ = 0.067
Ω = 24.1 r/s
ΩR = 722.55 ft/s
FLAPPING MODE
WITHOUT DYNAMIC INFLOW
WITH DYNAMIC INFLOW (PITT MODEL)
WITH DYNAMIC INFLOW (CARPENTER)
C_T = 0 0.00135 0.0054 0.0027 0.008
INFLOW MODE ON REAL AXIS
25
20
15
10
5
0
jω (r/s)
−30 −25 −20 −15 −10 −5
σ (1/s)

Fig. 5

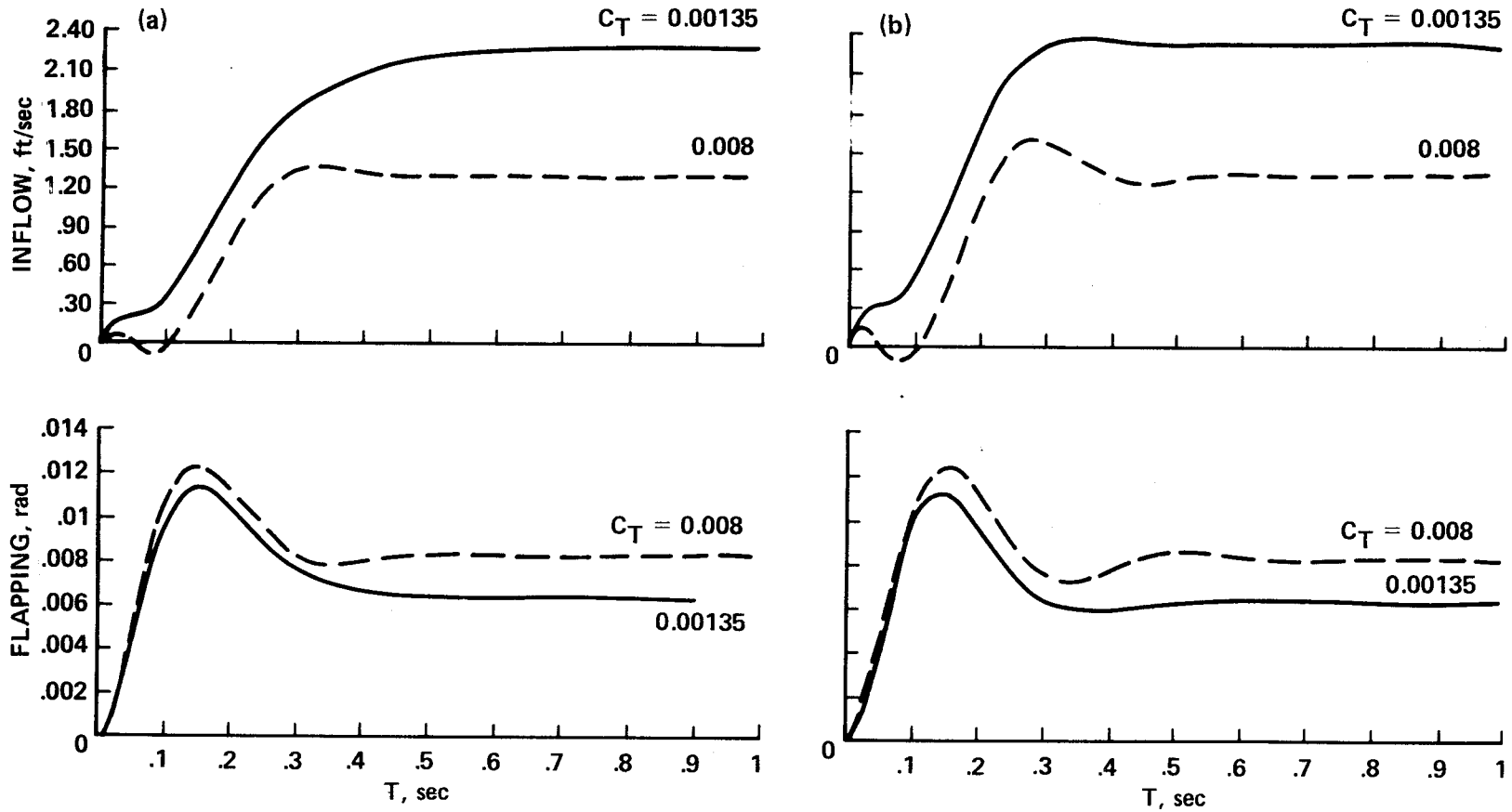
(a)
(b)
C_T = 0.00135
0.008
INFLOW, ft/sec
2.40
2.10
1.80
1.50
1.20
.90
.60
.30
0
FLAPPING, rad
.014
.012
.01
.008
.006
.004
.002
0
C_T = 0.008
0.00135
.1
.2
.3
.4
.5
.6
.7
.8
.9
1
T, sec

Fig. 6

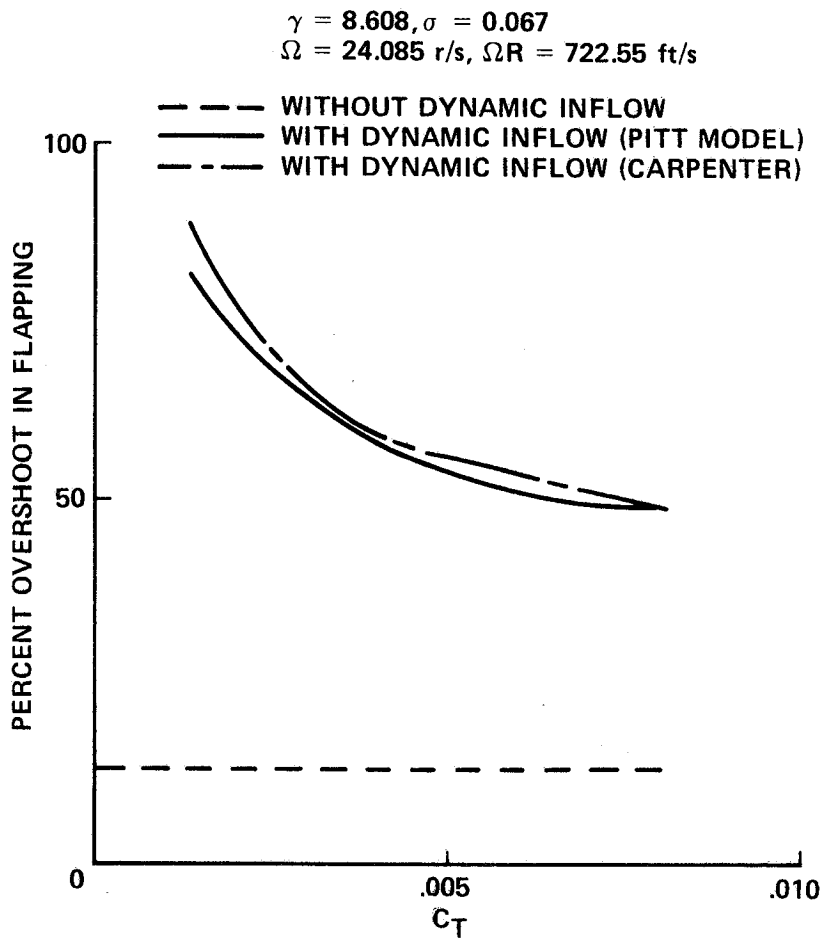
$\gamma = 8.608, \sigma = 0.067$
$\Omega = 24.085$ r/s, $\Omega R = 722.55$ ft/s
WITHOUT DYNAMIC INFLOW
WITH DYNAMIC INFLOW (PITT MODEL)
WITH DYNAMIC INFLOW (CARPENTER)
PERCENT OVERSHOOT IN FLAPPING
100
50
0
.005
.010
C_T

Fig. 7

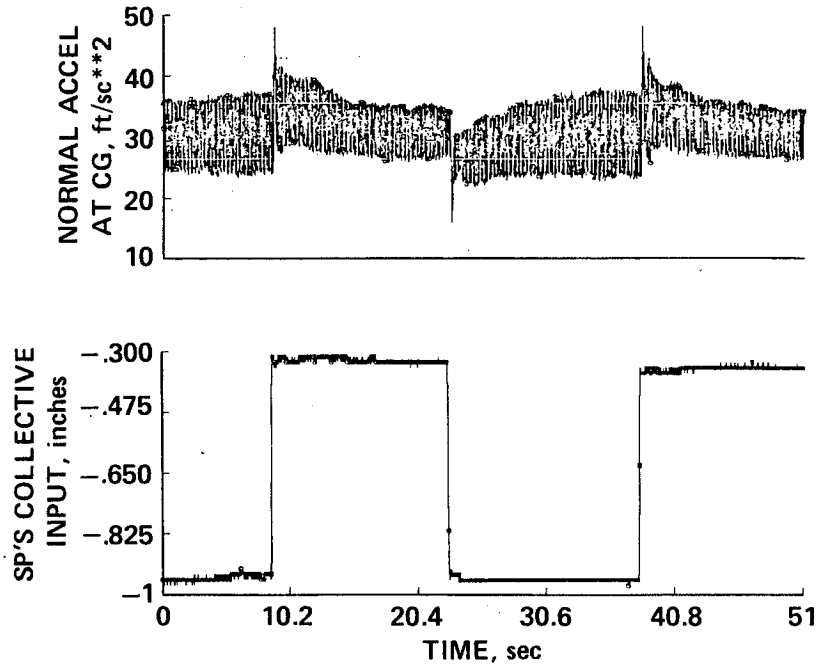
NORMAL ACCEL
AT CG, ft/sc**2
50
40
30
20
10
SP'S COLLECTIVE
INPUT, inches
−.300
−.475
−.650
−.825
−1
0
10.2
20.4
30.6
40.8
51
TIME, sec

Fig. 8

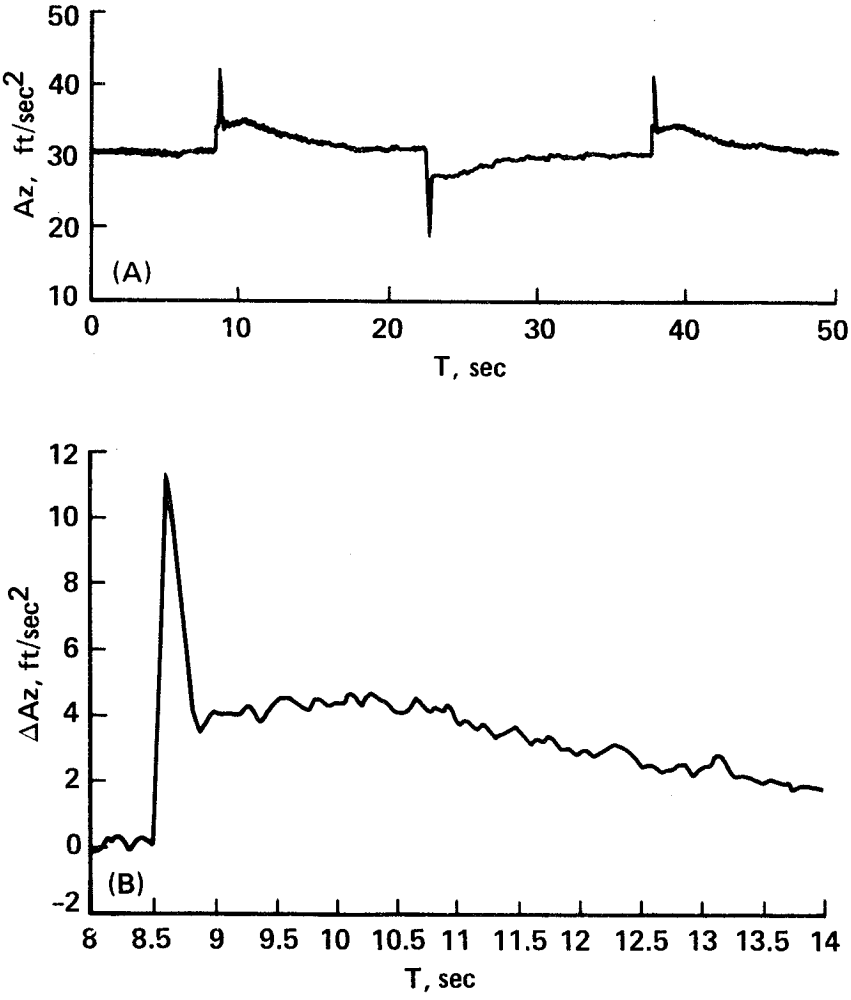
50
40
30
20
10
Az, ft/sec2
(A)
0
10
20
30
40
50
T, sec
12
10
8
6
4
2
0
-2
ΔAz, ft/sec2
(B)
8
8.5
9
9.5
10
10.5
11
11.5
12
12.5
13
13.5
14
T, sec

Fig. 9

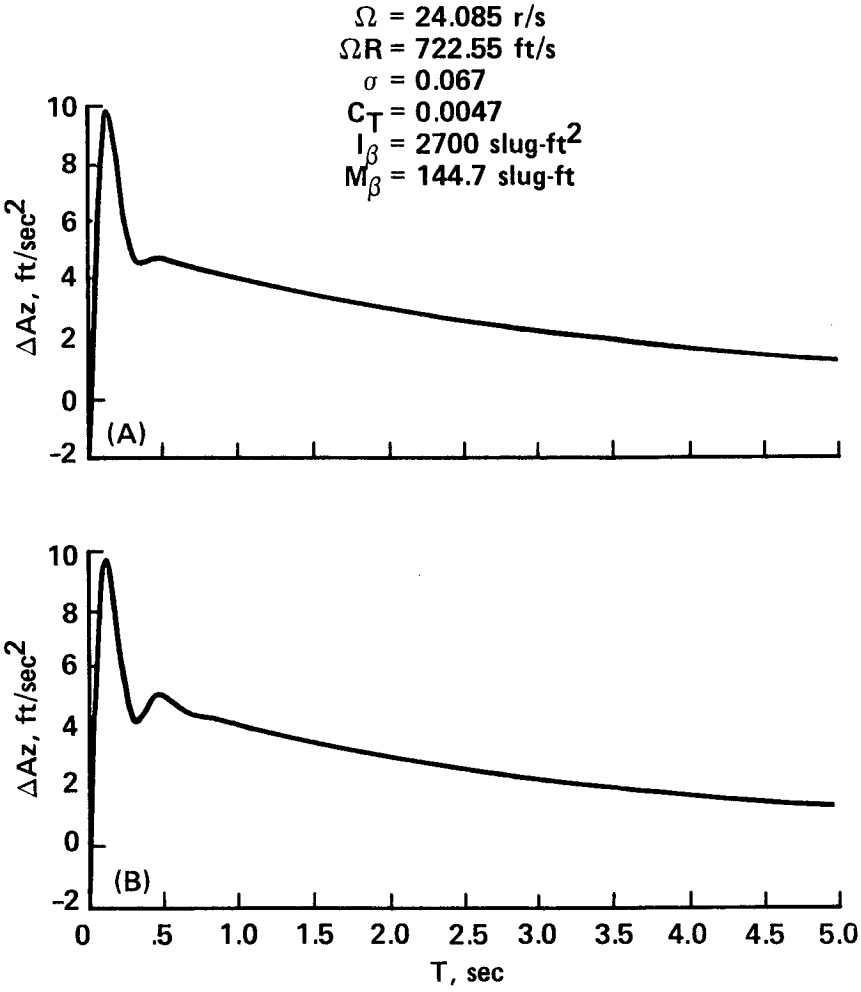
Ω = 24.085 r/s
ΩR = 722.55 ft/s
σ = 0.067
C_T = 0.0047
I_β = 2700 slug-ft^2
M_β = 144.7 slug-ft
ΔAz, ft/sec^2
(A)
(B)
T, sec

Fig. 10

Ω = 24.085 r/s
ΩR = 722.55 ft/s
σ = 0.067
C_T = 0.0047
I_β = 2700 slug-ft^2
M_β = 120.0 slug-ft
γ = 8.608

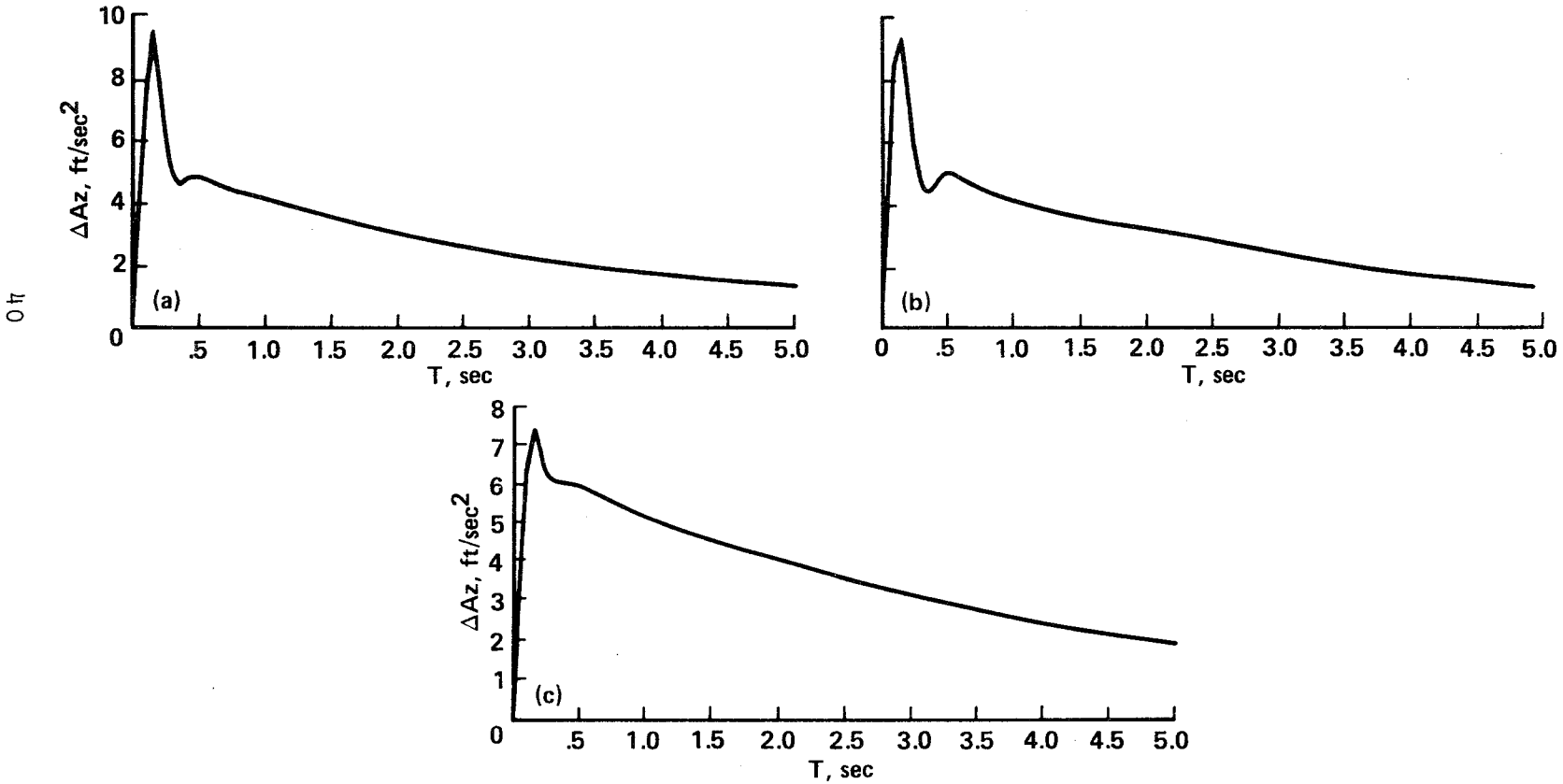

Fig. 11

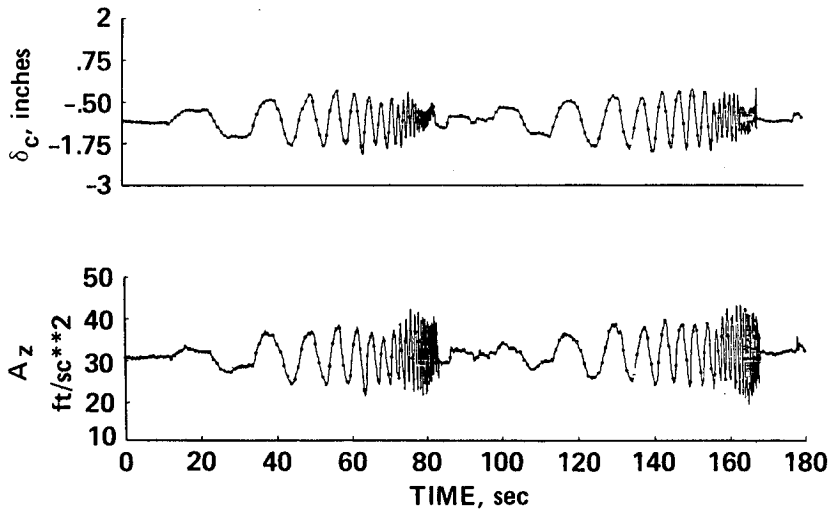
2
.75
-.50
-1.75
-3
δ_c, inches
50
40
30
20
10
Az
ft/sc**2
0
20
40
60
80
100
120
140
160
180
TIME, sec

Fig. 12

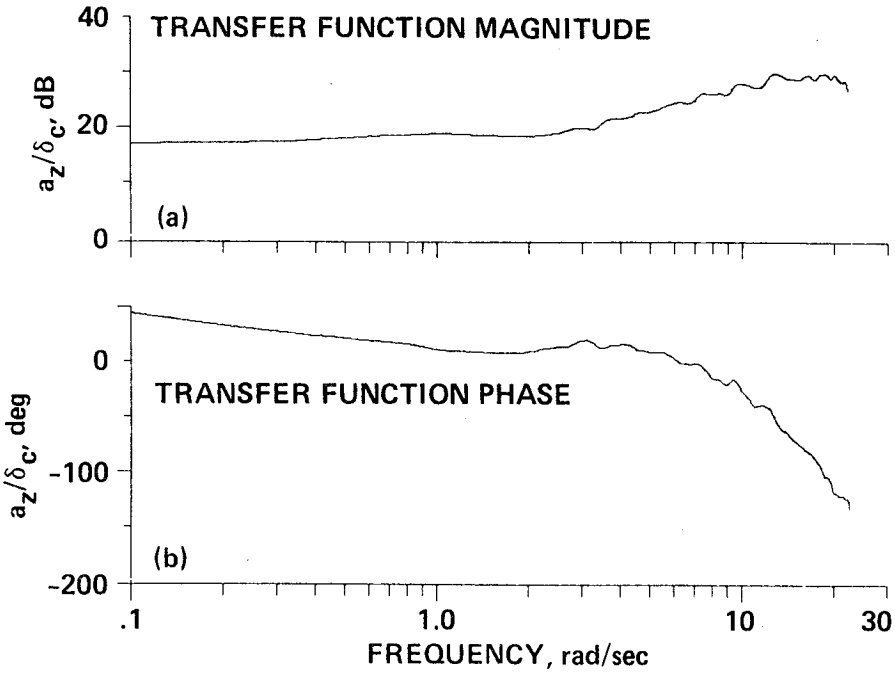
TRANSFER FUNCTION MAGNITUDE
40
20
0
a_z/δ_c, dB
(a)
TRANSFER FUNCTION PHASE
0
-100
-200
a_z/δ_c, deg
(b)
.1
1.0
10
30
FREQUENCY, rad/sec

Fig. 13

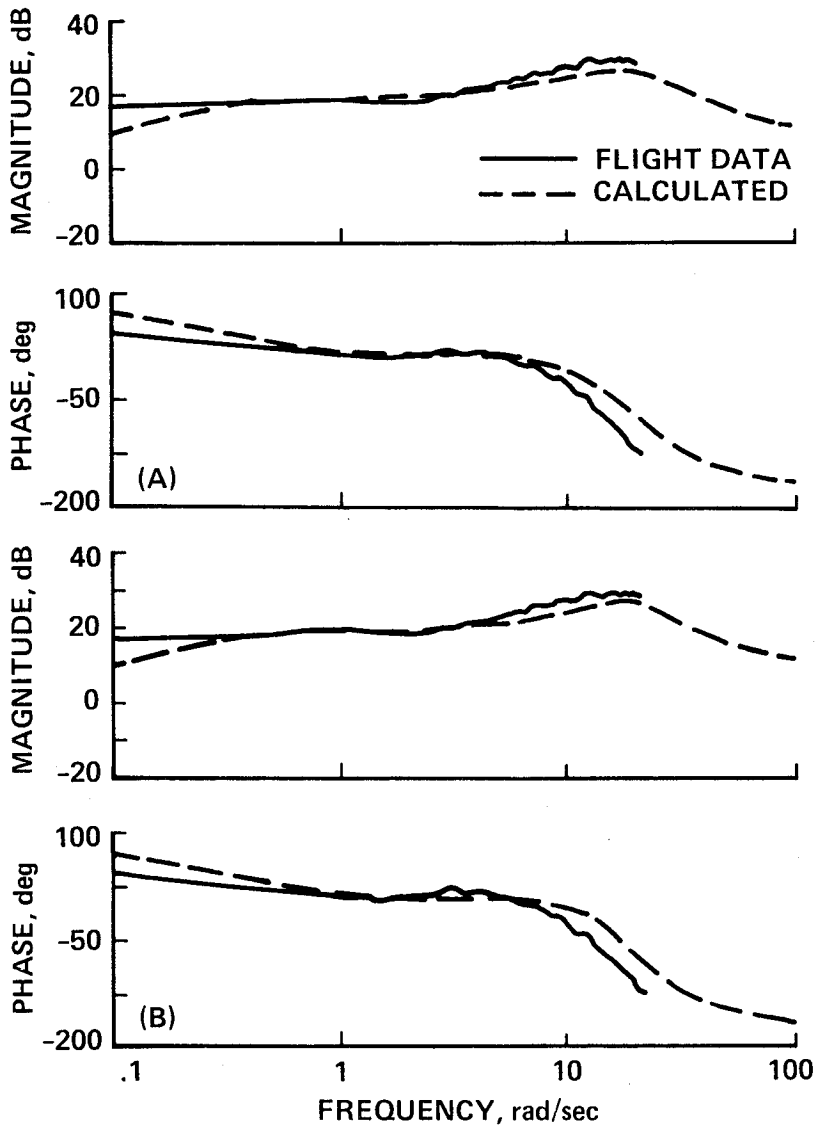
MAGNITUDE, dB
40
20
0
-20
FLIGHT DATA
CALCULATED
PHASE, deg
100
-50
-200
(A)
MAGNITUDE, dB
40
20
0
-20
PHASE, deg
100
-50
-200
(B)
.1
1
10
100
FREQUENCY, rad/sec

Fig. 14

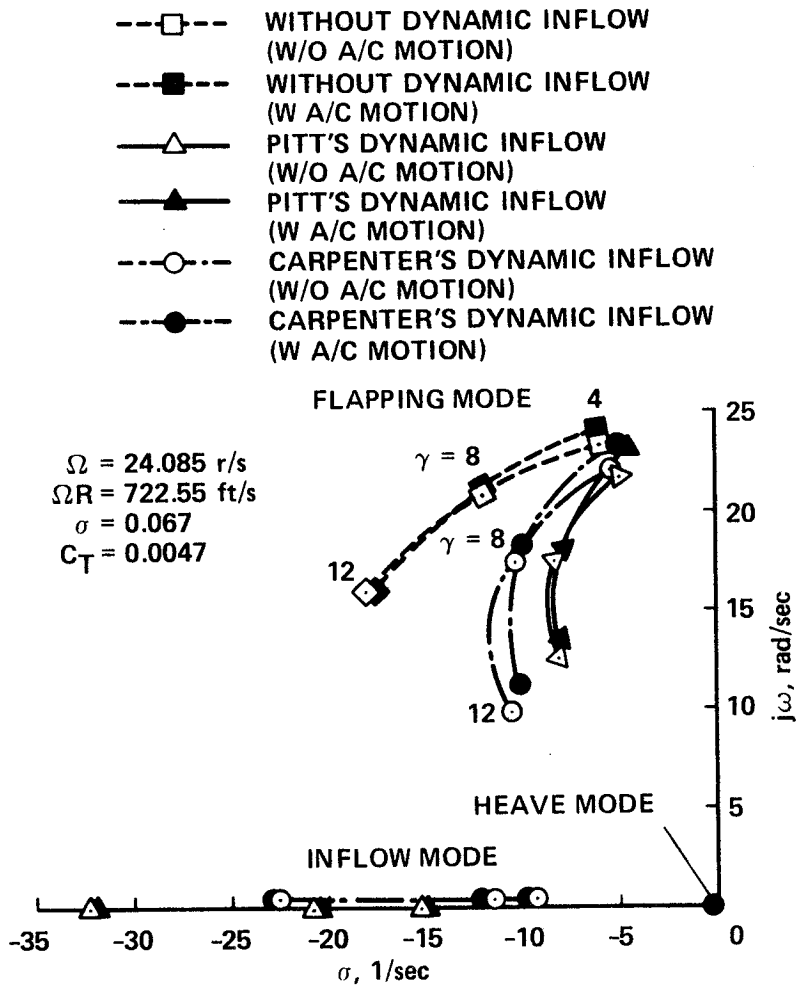
WITHOUT DYNAMIC INFLOW
(W/O A/C MOTION)
WITHOUT DYNAMIC INFLOW
(W A/C MOTION)
PITT'S DYNAMIC INFLOW
(W/O A/C MOTION)
PITT'S DYNAMIC INFLOW
(W A/C MOTION)
CARPENTER'S DYNAMIC INFLOW
(W/O A/C MOTION)
CARPENTER'S DYNAMIC INFLOW
(W A/C MOTION)
FLAPPING MODE
Ω = 24.085 r/s
ΩR = 722.55 ft/s
σ = 0.067
C_T = 0.0047
γ = 8
γ = 8
4
12
12
HEAVE MODE
INFLOW MODE
25
20
15
10
5
0
jω, rad/sec
-35
-30
-25
-20
-15
-10
-5
σ, 1/sec

Fig. 15

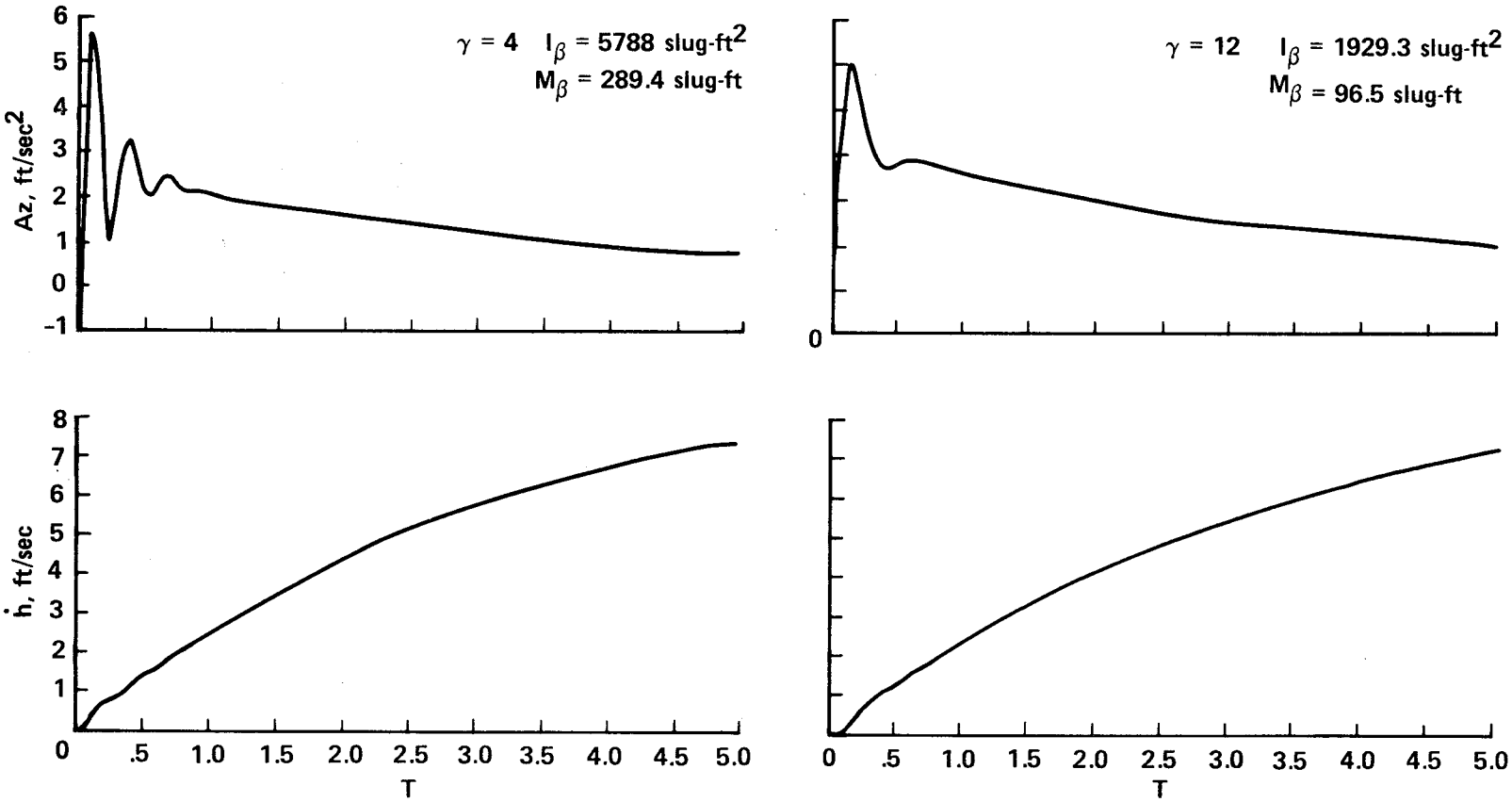
γ = 4 I_β = 5788 slug-ft^2
M_β = 289.4 slug-ft
γ = 12 I_β = 1929.3 slug-ft^2
M_β = 96.5 slug-ft
Az, ft/sec^2
ḣ, ft/sec
T
T

Fig. 16

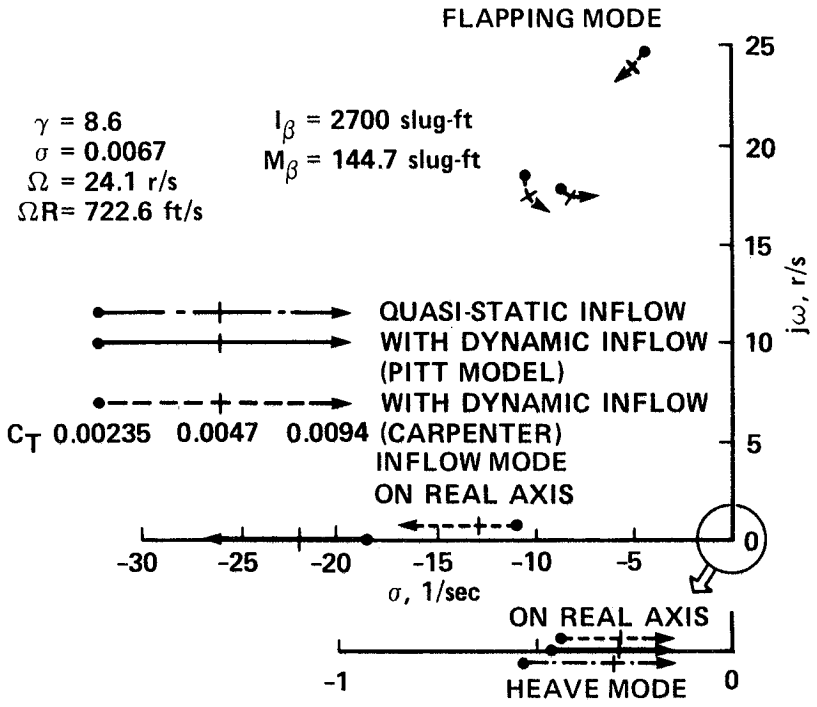
FLAPPING MODE
γ = 8.6
σ = 0.0067
Ω = 24.1 r/s
ΩR= 722.6 ft/s
I_β = 2700 slug-ft
M_β = 144.7 slug-ft
QUASI-STATIC INFLOW
WITH DYNAMIC INFLOW
(PITT MODEL)
WITH DYNAMIC INFLOW
(CARPENTER)
C_T 0.00235 0.0047 0.0094
INFLOW MODE
ON REAL AXIS
25
20
15
10
5
0
jω, r/s
-30 -25 -20 -15 -10 -5
σ, 1/sec
ON REAL AXIS
-1
HEAVE MODE
0

Fig. 17

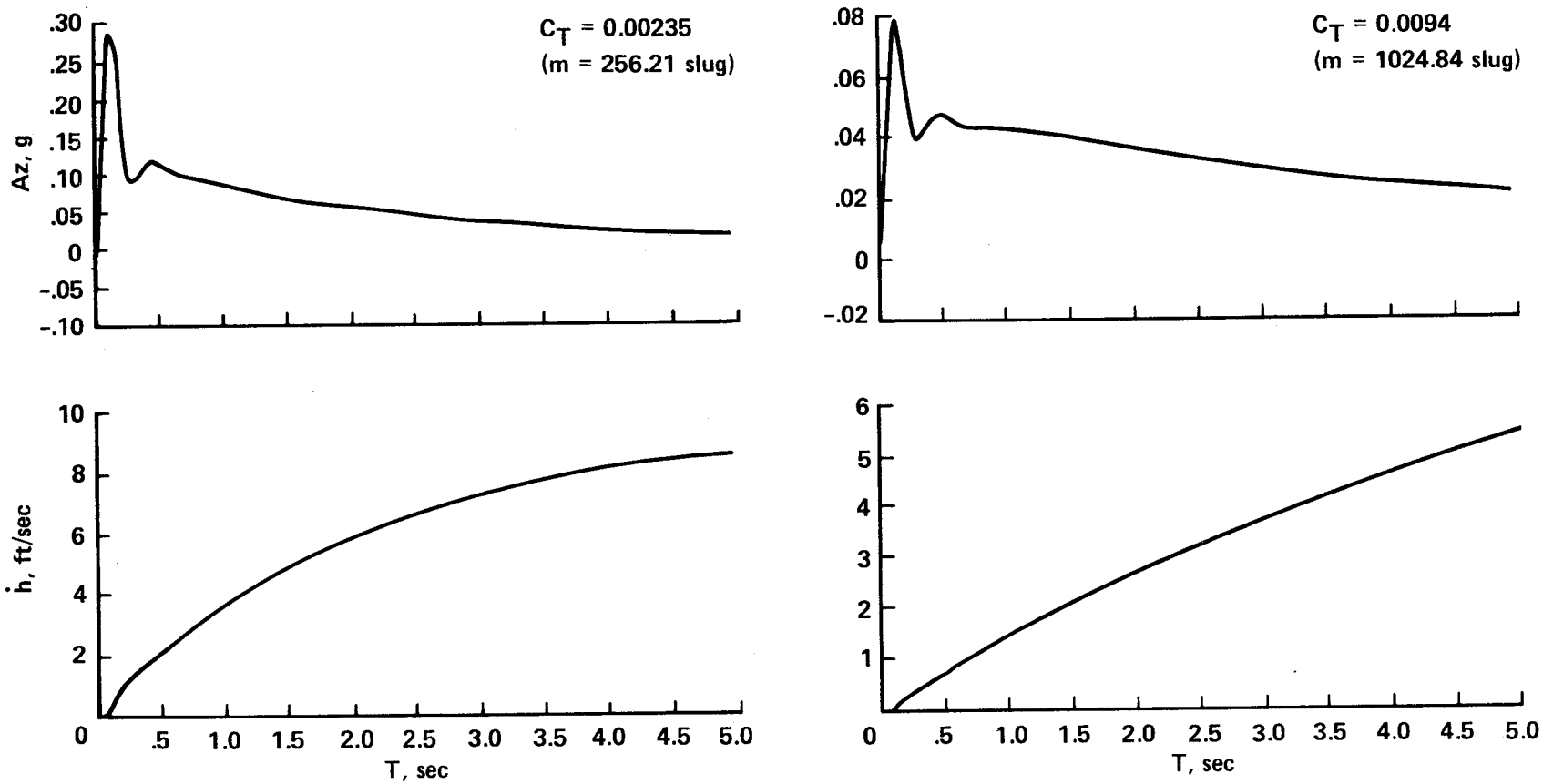
C_T = 0.00235
(m = 256.21 slug)
C_T = 0.0094
(m = 1024.84 slug)
Az, g
.30
.25
.20
.15
.10
.05
0
-.05
-.10
.08
.06
.04
.02
0
-.02
ḣ, ft/sec
10
8
6
4
2
0
6
5
4
3
2
1
.5
1.0
1.5
2.0
2.5
3.0
3.5
4.0
4.5
5.0
T, sec

Fig. 18

1. Report No.	2. Government Accession No.	3. Recipient's Catalog No.
NASA TM-88327		

4. Title and Subtitle	5. Report Date
INFLUENCE OF DYNAMIC INFLOW ON THE HELICOPTER VERTICAL RESPONSE	June 1986
	6. Performing Organization Code

7. Author(s)	8. Performing Organization Report No.
Robert T. N. Chen and William S. Hindson*	A-86262
	10. Work Unit No.

9. Performing Organization Name and Address	11. Contract or Grant No.
Ames Research Center, Moffett Field, CA 94035 *Stanford University, Stanford CA	

12. Sponsoring Agency Name and Address	13. Type of Report and Period Covered
National Aeronautics and Space Administration Washington, DC 20546	Technical Memorandum
	14. Sponsoring Agency Code 505-61-5

15. Supplementary Notes

Point of contact: Robert T. N. Chen, Ames Research Center, Moffett Field, CA 94035 (415)694-5008 or FTS 464-5008

16. Abstract

A study has been conducted to investigate the effects of dynamic inflow on rotor-blade flapping and vertical motion of the helicopter in hover. Linearized versions of two dynamic inflow models, one developed by Carpenter and Fridovich and the other by Pitt and Peters, were incorporated in simplified rotor-body models and were compared for variations in thrust coefficient and the blade Lock number. In addition, a comparison was made between the results of the linear analysis, and the transient and frequency responses measured in flight on the CH-47B variable-stability helicopter. Results indicate that the correlations are good, considering the simplified model used. The linear analysis also shows that dynamic inflow plays a key role in destabilizing the flapping mode. The destabilized flapping mode, along with the inflow mode that the dynamic inflow introduces, results in a large initial overshoot in the vertical acceleration response to an abrupt input in the collective pitch. This overshoot becomes more pronounced as either the thrust coefficient or the blade Lock number is reduced. Compared with Carpenter's inflow model, Pitt's model tends to produce more oscillatory responses because of the less stable flapping mode predicted by it.

17. Key Words (Suggested by Author(s))	18. Distribution Statement
Dynamic inflow Helicopter vertical response Stability and control Thrust response Flapping dynamics	Unlimited Subject category: 08

19. Security Classif. (of this report)	20. Security Classif. (of this page)	21. No. of Pages	22. Price*
Unclassified	Unclassified	47	A03

*For sale by the National Technical Information Service, Springfield, Virginia 22161